

## *Supporting Information for*

### **Chitosan nanoparticles for nitric oxide delivery in human skin**

M. T. Pelegriño,<sup>a,b</sup> R. Weller,<sup>c</sup> X. Chen,<sup>c</sup> J. S. Bernardes,<sup>d</sup> and A. B. Seabra<sup>b\*</sup>

<sup>a</sup>Exact and Earth Sciences Department, Universidade Federal de São Paulo, Rua São Nicolau, 210, CEP 09913-030, Diadema, SP, Brazil.

<sup>b</sup>Center of Natural and Human Sciences, Universidade Federal do ABC, Av. dos Estados 5001, CEP 09210-580, Santo André, SP, Brazil.

<sup>c</sup>Medical Research Council Centre for Inflammation Research, University of Edinburgh, Queen's Medical Research Institute, 47 Little France Crescent, Edinburgh, EH16 4TJ, UK.

<sup>d</sup>National Nanotechnology Laboratory (LNNano), National Center for Energy and Materials (CNPEM), Rua Giuseppe Máximo Scolfaro, 10.000, CEP 13083-970, Campinas, SP, Brazil .

## **EXPERIMENTAL SECTION**

### **Materials**

Chitosan (75% desacetylation), sodium tripolyphosphate (TPP), acetic acid, glutathione (GSH), 5,5'-dithiobis (2-nitrobenzoic acid) (DTNB), ethylenediaminetetraacetic acid (EDTA), sodium nitrite (NaNO<sub>2</sub>), 4,5-diaminofluorescein diacetate (DAF-2DA), phosphate buffer saline (PBS, pH 7.4), and ethanol were obtained from Sigma-Aldrich (St. Louis, MO, USA). The aqueous solutions were prepared using analytical grade water from a Millipore Milli-Q Gradient filtration system.

### **Synthesis of CS nanoparticles containing GSH**

CS nanoparticles (CS NPs) were prepared by ionotropic gelation process.<sup>1</sup> In brief, CS (2.6 mg·mL<sup>-1</sup>) and GSH (at concentrations of 26.7 or 266.7 mmol·L<sup>-1</sup>) were mixed through magnetic stirring in an aqueous solution of acetic acid (0.175 mol·L<sup>-1</sup>) for 90 min. TPP aqueous solution (0.6 mg·mL<sup>-1</sup>) was added dropwise in the CS/GSH suspension, following the volumetric proportion of 3CS/GSH: 1TPP. The final mixture was stirred for further 45 minutes at room temperature yielding a suspension of CS NPs containing GSH (final concentrations of GSH: 10 or 100 mmol·L<sup>-1</sup>), henceforth referred as GSH-CS NPs.

### **Dynamic light scattering measurements (DLS)**

DLS measurements were performed to determinate the average hydrodynamic diameter (assayed by % of number), size distribution, polydispersity index (PDI), and zeta potential of GSH-CS NPs by using the Nano ZS Zetasizer (Malvern Instruments Co, UK). Prior the analyses, the nanoparticle suspensions were filtered using a 0.45 µm membrane. The measurements were performed in three independent experiments, using a fixed angle of 173° in disposable folded capillary zeta cells with a 10 mm path length, in aqueous suspension at 25°C.

### **X-ray photoelectron spectroscopy (XPS)**

The surface composition of GSH-CS nanoparticles was analyzed by X-ray photoelectron spectroscopy (XPS), using a K-Alpha X-ray photoelectron spectrometer (Thermo Fisher Scientific, UK) equipped with a hemispherical electron analyzer and an aluminum anode X-ray source ( $K\alpha = 1486.6$  eV), providing an energy resolution  $\sim 1$  eV. Survey (*i.e.*, full-range) spectra were recorded using a pass energy of 200 eV and the atomic composition

of the samples was determined by integrating the core-level peaks, properly weighted by the photo-emission cross-section, using the Thermo Advantage software (Version 5.921).

### **Atomic force microscopy (AFM)**

Topography and phase contrast images of GSH-CS NPs were simultaneously obtained in a NX-10 Atomic Force Microscope (Park System) in tapping mode. A high resolution probe with 1 nm radius,  $K = 42 \text{ N m}^{-1}$  and resonance frequency within 260-320 kHz were used. Phase contrast imaging in AFM is able to detect viscoelastic dissipated property (chemical-dependent phase) and reveal more details about the surface. Prior to AFM imaging, 10  $\mu\text{L}$  of the of GSH-CS NPs dispersion was deposited on a silicon surface and let to dry by slow evaporation at room temperature. The scanning system is enclosed within an environmental chamber under controlled temperature and relative humidity.

### **GSH encapsulation efficiency in CS NPs**

The encapsulation efficiency of GSH in CS NPs was measured by the titration of free thiol group of GSH with DTNB.<sup>1,2</sup> Briefly, a volume of 500  $\mu\text{L}$  of aqueous suspension of GSH-CS NPs was filtered in a Microcon centrifugal filter device (MWCO 10,000, Millipore). A volume of 0.25 mL of free GSH solution, eluted from the centrifugal filter device, was added to 1.2 mL of 0.7  $\text{mmol}\cdot\text{L}^{-1}$  of aqueous solution of DTNB, in PBS solution (pH 7.4), containing 10.3  $\text{mmol}\cdot\text{L}^{-1}$  EDTA. After 5 min of incubation, the absorbance at 412 nm ( $\epsilon = 14.15 \text{ mmol}^{-1}\cdot\text{L}\cdot\text{cm}^{-1}$ ) was measured in the UV-vis spectrophotometer Agilent 8453 (Palo Alto, CA, USA). The measurements were performed in duplicates and the percentage of encapsulated GSH was calculated by the Eq. 1.

$$\text{Encapsulation efficiency (EE\%)}: \left[ \left( \frac{\text{total GSH} - \text{free GSH}}{\text{total GSH}} \right) \times 100 \right] \quad (\text{Eq. 1})$$

### **Nitrosation of encapsulated and free GSH yielding GSNO**

Free thiol groups of encapsulated GSH were nitrosated directly in the CS NPs suspension by adding equimolar amount of sodium nitrite (NaNO<sub>2</sub>), in acidified medium (pH ~ 4). The final suspension was stirred for 45 min, protected from light, in an ice bath. The formation of GSNO in CS NPs was confirmed by the appearance of the characteristic S-NO group absorption bands at either 336 nm ( $\epsilon = 980.0 \text{ mol}^{-1} \cdot \text{L} \cdot \text{cm}^{-1}$ ) or at 545 nm ( $\epsilon = 18.4 \text{ mol}^{-1} \cdot \text{L} \cdot \text{cm}^{-1}$ ) using the UV–vis spectrophotometer Agilent 8453 (Palo Alto, CA, USA).<sup>1,2</sup> Similarly, free GSNO was synthesized by adding equimolar amount of NaNO<sub>2</sub> to GSH aqueous solution, in acidified medium.<sup>3</sup> The obtained GSNO was precipitated by the addition of acetone, filtrated and washed with cold water. The obtained solid was freeze–dried for 24 h.

### ***In vitro* GSNO release from free GSNO and from GSNO-CS NPs**

The *in vitro* kinetics of intact GSNO release from free GSNO in aqueous solution and from GSNO-CS NPs were performed by using a Franz diffusion cell (standard cell, 15 mm of diameter, 7 mL, Hanson Research Corporation).<sup>4</sup> This cell consists of donor and receptor chambers, separated by a polysulfone membrane disc filters with a 450 nm pore size (Tuffryn, Pall Corporation, Port Washington, NY, USA). The donor compartment was filled with 2.5 mL of free GSNO in PBS or with aqueous suspension of GSNO-CS-NPs, in both cases the initial GSNO concentration was 10 mmol·L<sup>-1</sup>. The receptor compartment was filled with PBS at pH 7.4 and kept under magnetic stirring at 32.5 ± 0.5°C. The entire cell was protected from room light. A volume of 500 µL was withdrawn from the receptor compartment, in 30 min intervals, and replaced by an equivalent volume

of fresh PBS. The withdrawn samples were immediately analyzed by Uv-visible spectrophotometry. The amount of intact GSNO released through the membrane was determined by monitoring the spectral changes at 336 nm ( $\epsilon = 980 \text{ mol}^{-1} \cdot \text{L} \cdot \text{cm}^{-1}$ ), due to the presence of GSNO.<sup>5</sup> The total GSNO released after 4.5 h of monitoring was quantified by integrating the GSNO concentration at the receptor compartment *versus* time, in the obtained curves, as previously described.<sup>6</sup> The results were reported as the mean  $\pm$  standard deviation (SD) of three independent experiments and expressed in terms of the GSNO percentage for the release experiments. In order to investigate the mechanism of GSNO release from free GSNO and from GSNO-CS NPs through the membrane, the Higuchi mathematical model were applied to the kinetic curves (Eq. 2).<sup>2,7,8</sup>

$$Q_t = K_H t^{0.5} \quad (\text{Eq. 2})$$

Where  $Q_t$  is the cumulative amount of GSNO released at time  $t$ ,  $K_H$  is the release constant, and  $t$  is time. The results were adjusted through linear regression and correlation coefficient ( $r^2$ ) analyzed.<sup>9</sup>

### **NO permeation in *ex vivo* human skin sections from GSNO-CS NPs in the dark and under UV irradiation**

Redundant skin from abdominoplasty procedures was snap frozen and cut in sections (10 mm<sup>2</sup> and 5 mm), which were incubated with 10 mmol·L<sup>-1</sup> of the NO fluorochrome DAF-2DA, for 24 hours at 37°C.<sup>10</sup> A volume of 200  $\mu\text{L}$  of aqueous suspension of freshly prepared GSNO-CS NPs (GSNO concentration of 100 mmol·L<sup>-1</sup>) was applied onto the *stratum corneum* surface of skin sections ( $n = 6$ ), covering only the epidermis to mimic a

dermatological application, and incubated for 6 hours at 37°C. GSH-CS NPs (GSH concentration of 100 mmol·L<sup>-1</sup>) and untreated skin sections were used as control groups (n = 6 for each group). After this incubation, the sections were washed several times with PBS to completely removed the NP suspensions, and: (i) irradiated with UV light at 290 nm for 20 minutes (6.5 J·cm<sup>2</sup>), or (ii) keep in the dark. After this, the skin sections were immediately frozen with liquid nitrogen. All the skin sections were cut into 8 μm sections by microtome and analyzed using a confocal microscope (Leica SP5C spectral confocal laser scanning microscope, Wetzlar, Germany). The fluorescence intensities due to the presence of NO in the skin sections were quantified using Image-Pro Plus (Media Cybernetics, Rockville, MD).

#### **Data and statistical analysis**

Data were analyzed using Graph Pad Prism 5 (La Jolla, CA) and expressed as means ± SEM. Differences were compared by one-way analysis of variance, after Tukey's correction for multiple comparisons. P < 0.05 was considered statistically significant.

#### **RESULTS AND DISCUSSION**

Figure S1 shows a representative size distribution curve (A) of the GSH-CS NPs obtained by DLS measurements, and the corresponding autocorrelation curve (B), showing monodal size distribution. In addition, the autocorrelation curve shows that there is no deviation by the end of the correlation, indicating the absence of contaminants, sedimentations and agglomerations. Moreover, the intercept point (y-axis) is between 0.8 and 1.0, indicating an acceptable counting for the size estimation of the nanoparticles.

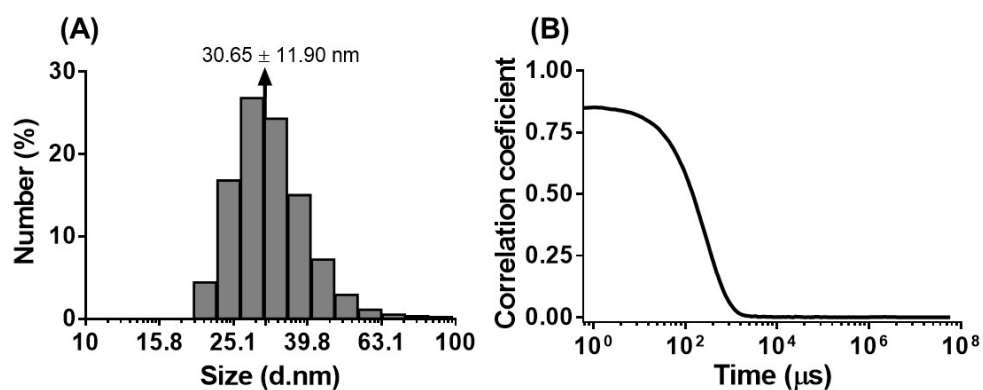


**Figure S1.** Representative size distribution curve of GSH-CS NPs (A) and the autocorrelation curve (B), assayed by DLS measurements.

Chemical surface composition of GSH-CS NPS was acquired by XPS and then compared to the total composition of the system (Table S1).

**Table S1.** Chemical surface composition of GSH-CS NPs measured by XPS

Chemical Element	Atomic % (point 1)	Atomic % (point 2)	Atomic % (point 3)
O1s	25.61	26.39	26.16
C1s	56.51	52.55	54.43
N1s	12.85	12.67	13.72
S2p	3.89	3.87	3.65
Na1s	0.39	0.47	0.42
P2p	0.46	0.76	0.62

The proposed nanostructure model for GSH-CS NPS is shown in Figure S2.

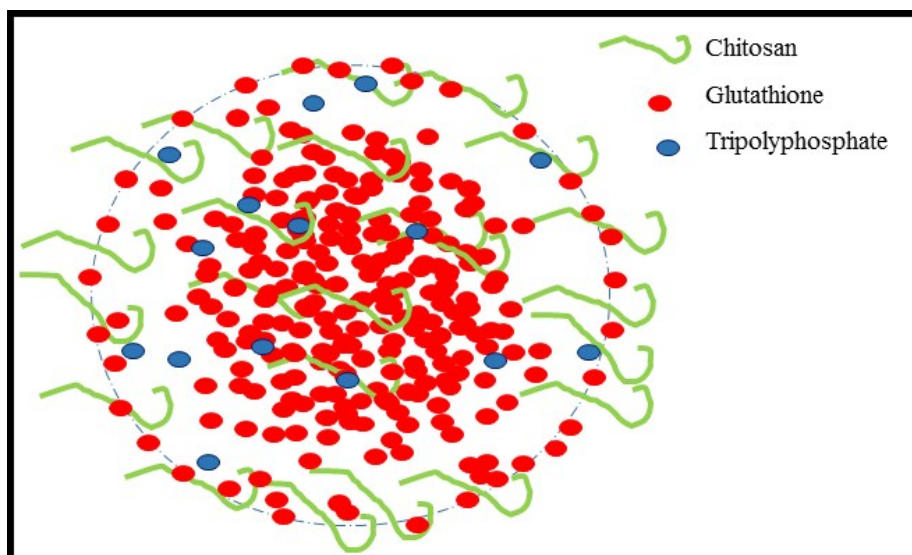


**Figure S2.** Scheme showing the proposed core-shell nanostructure of GSH-CS NPs. The red and blue circles correspond to, respectively, GSH and TPP. The dotted line represents the shape of the nanoparticle and the green lines represent the chitosan chains.

## REFERENCES

1. V. F. Cardozo, C. A. C. Lancheros, A. M. Narciso, E. C. S. Valereto, R. K. T. Kobayashi, A. B. Seabra and G. Nakazato, *Int. J. Pharm.*, 2014, **473**, 20–29.
2. P. D. Marcato, L. F. Adami, R. de M. Barbosa, P. S. Melo, I. R. Ferreira, L. de Paula, N. Duran and A. B. Seabra, *Curr. Nanosci.*, 2013, **9**, 1–7.
3. N. M. Silveira, L. Frungillo, F. C. C. Marcos, M. T. Pelegrino, M. T. Miranda, A. B. Seabra, I. Salgado, E. C. Machado and R. V. Ribeiro, *Planta*, 2016, **244**, 181–190.
4. T. J. Franz, *J. Invest. Dermatol.*, 1975, **64**, 1975.
5. A. B. Seabra and M.G. de Oliveira, *Biomaterials*, 2004, **25**, 3773–3782.
6. R. Vercelino, T. M. Cunha, E. S. Ferreira, F. Q. Cunha, S. H. Ferreira and M. G. de Oliveira, *J. Mater. Sci: Mater. Med.*, 2013, **24**, 2157–2169.
7. A. C. S. Akkari, E. V. R. Campos, A. F. Keepler, L. F. Fraceto, E. Paula, G. R. Tófoli and D. R. Araújo, *Colloids Surf. B Biointerfaces*, 2016, **138**, 138–147.

8. R. W. Korsmeyer, R. Gurny, E. Doelker, P. Buri and N. A. Peppas, *Int. J. Pharm.*, 1983, **15**, 25–35.
9. P. Costa and J. M. S. Lobo, *Eur. J. Pharm. Sci.*, 2001, **13**, 123–133.
10. D. Liu, B. O. Fernandez, A. Hamilton, N. N. Lang, J. M.C. Gallagher, D.E. Newby, M. Feelisch and R. B. Weller, *J. Invest. Dermatol.*, 2014, **134**, 1839-1846.